



Stockholm
University

Bachelor Thesis

Degree Project in
Geology 15 hp

Evaluating melt genesis and formation of Socotra high silica rhyolites using major and trace elements

Samuel Clark



Stockholm 2014

Department of Geological Sciences
Stockholm University
SE-106 91 Stockholm

Abstract

Formational mechanisms of HSRs are a debated topic. There are various theories concerning the origin and formation. In this paper the two theories interstitial melt extraction (Bachmann and Bergantz 2004) and Partial melting of a mafic parent (Streck and Grunder 2008) are discussed. High Silica rhyolites from the Island of Socotra have undergone whole rock analysis using XRF and ICP. Major and minor trace element data is used in order to evaluate melt genesis and formation of Socotra high silica rhyolites using a series of geochemical plots and classification methods. Various REE, multi-element and other diagrams were used to determine which theory the Socotran high silica rhyolites formed by. The HSR's showed typical characteristics of their classification, such as depletion in Eu, Sr and Ba but enrichment in remaining REE's. Two different groups of rhyolite origin were distinguished. One formed of Calc-Alkaline HSR, that was shown to originate from the Bachmann and Bergantz (2004) melt-mush model, and the other of rhyolites of Tholeiitic origin and composition.

Table of contents

<u>Abstract</u>	1
<u>Table of contents</u>	2
<u>1 Introduction</u>	3
<u>2 Background</u>	4
2.1 High Silica Rhyolites	4
2.2 High silica rhyolite formation	4, 5
2.3 Geological setting	5, 6, 7
2.4 -Local geological settings	8
2.4.1 Field relationships	8
2.5 Sample collection	9
2.6 Analytical methods and data limitations	10
<u>3 Data analysis</u>	11
3.1 Classification	11
3.2 Loss On Ignition (LOI)	11, 12
<i>Table 1 – Major and trace element</i>	13
3.3 Thin sections-High Silica Rhyolite	14
<u>4 Geochemical results</u>	15
4.1- $\text{Na}_2\text{O}+\text{K}_2\text{O}$	15
4.2 Oxide vs SiO_2 Plots	16
4.3- CIPW-Normalisation	17
<i>Table 2- Results table of CIPW norm</i>	18
4.4- Rare Earth Elements	19
4.5 Multi element plot	20
4.6 Europium	21
<u>5. Discussion</u>	22
5.1 Sample classification	22
5.2 Geochemical groups	22
5.2.1 Sr v Y	22
5.2.2 Rb vs Sr	23
5.3 Formational processes	24
5.3.1 Rare earth elements-revisited	24
5.3.2 Formational Model	25
<u>6 Conclusion</u>	26
<u>7 Reference list</u>	27, 28

1 Introduction

This study aims to evaluate the genesis and formation of high silica rhyolites from the Island of Socotra. This will involve the use of major and trace element geochemical data, which has been obtained by geochemical analysis, to make conclusions regarding high silica rhyolite (HSR) genesis. The data used in this study was collected from the Island of Socotra. The island of Socotra is located within a small archipelago of four islands in the Indian Ocean, shown in figure 1. The island is situated around 240 kilometres east of the Horn of Africa and 380 kilometres south of the Arabian Peninsula. Rock samples were collected from various localities on the island, shown in figure 1. The rock samples were taken back to the lab to undergo geochemical analysis using XRF and ICP. Formational mechanisms of HSRs remain an area of debate today. Once having undergone geochemical analysis, the results will be presented, discussed and conclusions drawn on the origin of the high silica rhyolites. Thin sections will also be briefly discussed along with field relationships. Two different theories of high silica rhyolite formation will be tested and we can hypothesise that the geochemical data will show one of these two models to be correct.

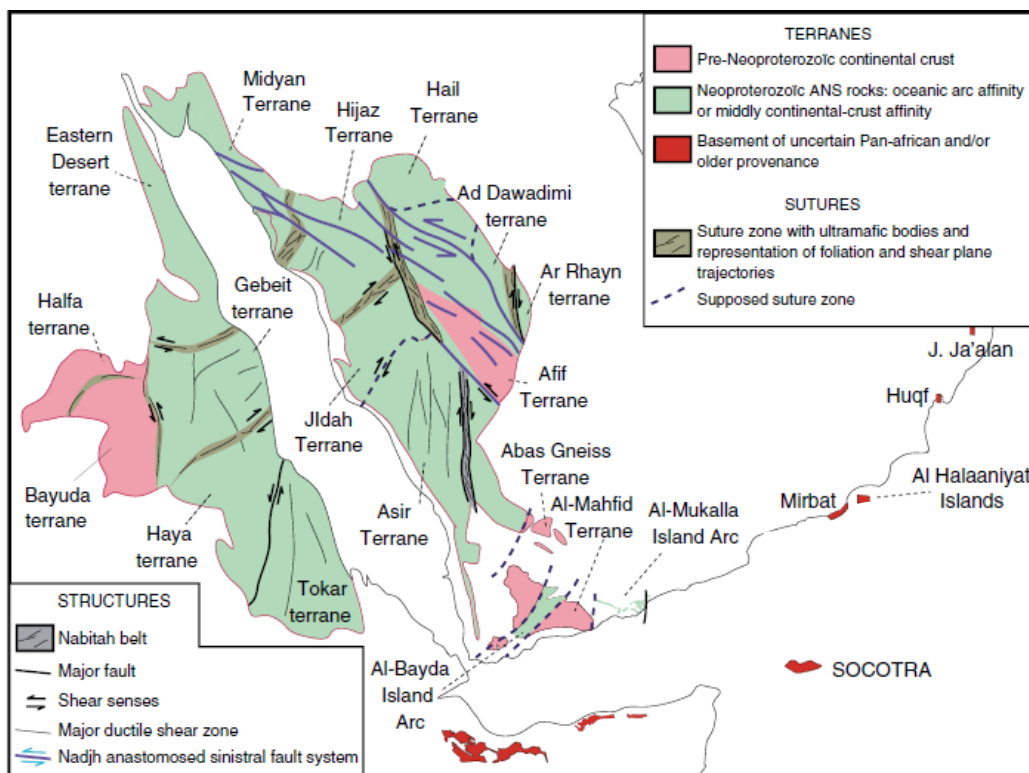


Figure 1 – Map showing location of Socotra (Denèle et al., 2013)

2 Background

2.1 High Silica Rhyolites

High silica rhyolites are an extrusive volcanic rock, which as their name states, have high silica content. High silica rhyolites form from very viscous high silica melts due to their high silica and low Iron and magnesium values and are typically for phenocryst poor (Glazner. Et al. 2008)(Streck and Grunder. 2008) This is due to the fact that they are so evolved that they are chemically limited in regards to mineralogy. High silica rhyolites can form in a range of geological settings, including all except ocean rifting, and typically form some of the largest eruptions in history (Mason et al. 2004). They generally found in geological settings where there are voluminous intermediate rocks and in bimodal provinces.

High silica rhyolites (HSR's), despite being an extrusive volcanic rock, do not share the same characteristics as a usual rhyolite and can form under unique processes. High silica rhyolites can be recognized from the geochemical data due to their distinct geochemical signature. HSR's are classified as such due to a SiO₂ wt% of >75%, a very high silica content. Furthermore HSR's show an enrichment in all REE's, with the exception of Eu. They are also depleted in Sr and Ba. These three elements are feldspar-compatible elements. Low Ba, Sr, Eu element abundances require extensive fractional crystallization of feldspar-rich assemblages which is inconsistent with partial melting of most crustal rocks (Glazner. Et al 2008). This means Rb/Sr ratios seen are usually much higher in silica rich igneous rocks (Halliday 1991). This specific geochemical signature will be tested for in this study.

2.2 High silica rhyolite formation

How High Silica Rhyolites form remains a point of discussion and debate today. In this study, two current theories will be discussed and certain criteria supporting those theories will be evaluated. The first is the formation of HSR through Extremely fractionated melts, where interstitial residual melt is extracted from crystalline mush of intermediate bulk composition. This was proposed by Bachmann and Bergantz (2004). The other theory is the Re-melting of mafic-intermediate rocks followed by protracted crystallization, proposed by Streck and Grunder (2008).

According to Bachman and Bergantz (2004), crystal poor rhyolites are formed after being extracted from batholithic crystal mushes. This melt expulsion model requires upward percolation of buoyant interstitial melt away from a crystal mush (Bachman and Bergantz 2004). For magmatic evolution through fractional crystallisation to occur, differential motion between the crystals is required, however there is no consensus in literature on the dominant processes occurring in silicic magma systems.

In general, silicic volcanics are linked to large volume-shallow granitoids (Bachmann and Bergantz 2004). HSRs are thought to form in the following way. Crystals are initially held in suspension at crystallinities of <45% crystals and are convecting. As fractionation continues the crystals reach 45-50%. At these crystallinities the interstitial melt is rhyolitic in composition i.e.- has a high silica content. When these crystallinities are reached the magma in the chamber can no longer convect and comes to a complete halt. This allows melt extraction to begin by several processes. (Bachmann and Bergantz 2004). As this interstitial melt percolates upwards, it begins to form a rhyolitic horizon at the roof of the chamber. This rhyolitic horizon is a crystal poor melt-cap at the top of granodioritic magma chamber. This is then erupted and forms a high silica rhyolite rock. The

erupted rocks typically have a calc-alkaline association and require extremely voluminous magma batches (Streck and Grunder 2008).

It is important to note that this model involves the process of fractional crystallisation. It is therefore supported by the typical geochemistry of high silica rhyolites as they typically have Eu, Sr and Ba depletions which are consistent with fractional crystallisation of feldspar and in general HSR suits contain highly fractionated magmas (Halliday 1991). Overall in this model, rhyolites form by separation of rhyolitic liquid from the crystal mush that forms granodioritic and granitic plutons.

The second model is one proposed by Streck and Grunder(2008), considers the origin of rhyolites associated with tholeiitic basalt in bimodal provinces. While the most evolved rhyolites are compositionally virtually indistinguishable from those of calcalkaline suites, the parental rhyolites from bimodal suites are more Fe-rich than their calcalkaline counterparts. In this model it is proposed that rhyolites can form from a mafic parent that has undergone 5-20% melting. This small amount of re-melting enables a high silica melt to form which can essentially be erupted to form High silica rhyolites. The high silica rhyolites produced have different geochemical characteristics than those extracted from crystal mush. They commonly have Fe-enriched characteristics with typically only a single feldspar shown in the rock. Due to the fact that they form from the re-melting of a mafic parent, it can be inferred that they would be rich in incompatible elements. This means that Ba and Sr would be more enriched. Also Eu would not show depletion in this model. The HSR's would also show a stronger decrease in Ba compared to Sr due to the different fractionation of plagioclases.

In this theory it is discovered that crystal fractionation processes within rhyolites can ultimately lead to daughter rhyolitic compositions that are virtually indistinguishable from calc alkaline crystalline mush. This emphasizes the point that for the discussion of howHSRs are generated it is of great importance to keep in mind the degree of evolution of the erupted rhyolite because prior protracted fractionation may obscure its rhyodacitic to rhyolitic ancestry (Streck and Grunder 2008).

It is clear to see, from these two theories, that the crystallisation of is critical to determine a melts evolution and genesis.. In this study the crystallisation of plagioclase will be discussed and the different chemical signatures for each theory will be observed.

2.3 Geological setting

The Island of Socotra is located in the north western region of the Indian Ocean as previously shown shown in figure 1. The Island forms part of the Socotran archipelago, around 200km east of the tip of the horn of Africa and 280km south from the cost of Yemen. The Island was originally part of Gondwana and and detached during the Miocene epoch, in the same set of rifting events that opened the Gulf of Aden to its northwest, meaning the Island belongs to the southern rifted margin of the Gulf of Aden which is an active oceanic basin (Leroy et al. 2004).

The gulf of Aden was created by processes of oblique rifting, between the Somalia plate and Arabian plate (Beydoun and Bighan 1969). Rifting began around 35 Ma and oceanic accretion is recorded from 17.6 Ma along the whole Gulf of Aden (Denele et al. 2013).The islands geology can be divided into three main regions; The Haggier Mountains, the limestone plateau (permeated with karstic caves)and the alluvial coastal plains (Figure 2). These main rock types correspond to three basement highs located at the head of tilted blocks. The most voluminous basement outcrop, the Mont-Haggier basement high is located at the eastern part of the island. The oldest rocks lie at the

base of the sequence as the Neoproterozoic basement shown in figure 3. Neoproterozoic basement of Socotra displays a great variety of metamorphic, plutonic and volcanic rocks. The base of the section (the oldest part) is made up of amphibolite facies meta-sediments and meta-igneous rocks. These are Precambrian in age and are formed up of polyphase schists, ortho and paragenesis, intruded by syn-late kinematic foliated granites and late-kinematic gabbro, as well as by early paleozoic lavas and pyroclastic rocks within the haggier intrusive complex. Post-kinematic igneous activity gave rise to a sequence of volcanic rocks, hornblende/biotite and peralkaline granites, gabbros and minor intrusions, which make up the bulk of the Haggier mountains. Above these lie unconformable sediments from the Mesozoic to quaternary period. This is a Precambrian unconformity and sediments formed in shallow seas from Cretaceous limestone, Palaeocene-Eocene limestone and Oligocene-Miocene chalk lie in order from oldest to youngest. Above these, sediments of Mesozoic and younger age lie unconformably on the basement. This is a Precambrian unconformity and sediments formed in shallow seas include Cretaceous limestone, Palaeocene-Eocene limestone and Oligocene-Miocene chalk, from oldest to youngest. Above these another unconformity occurs at the Pleistocene where Pleistocene and Holocene heterogeneous marine, fluvial and continental deposits are found. A summary of the sequence can be seen in figure 3. It is important to note that the basement is exposed throughout the island in small and isolated regions near sea level. Basement rocks are of 860-720 Ma. There are a lot of Haggier dykes that extend from the mountainous region which can be seen by several localities in figure 7.

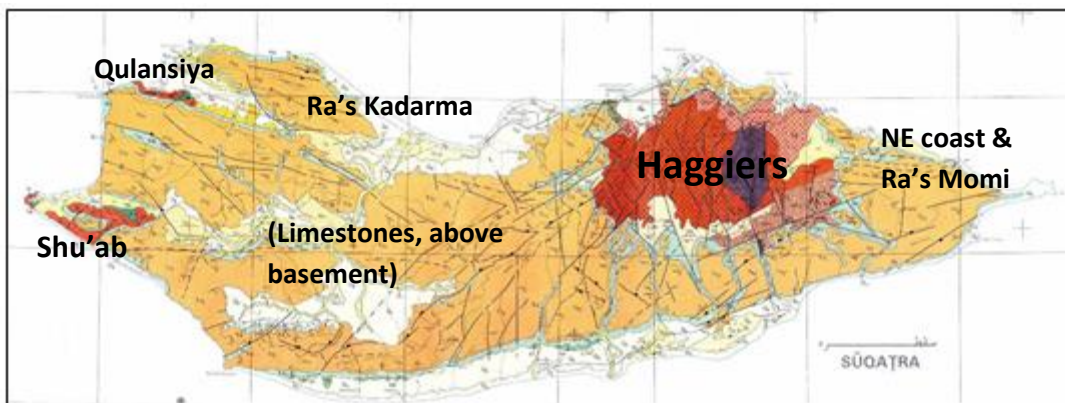


Figure 2-The different geological regions of the island of Socotra

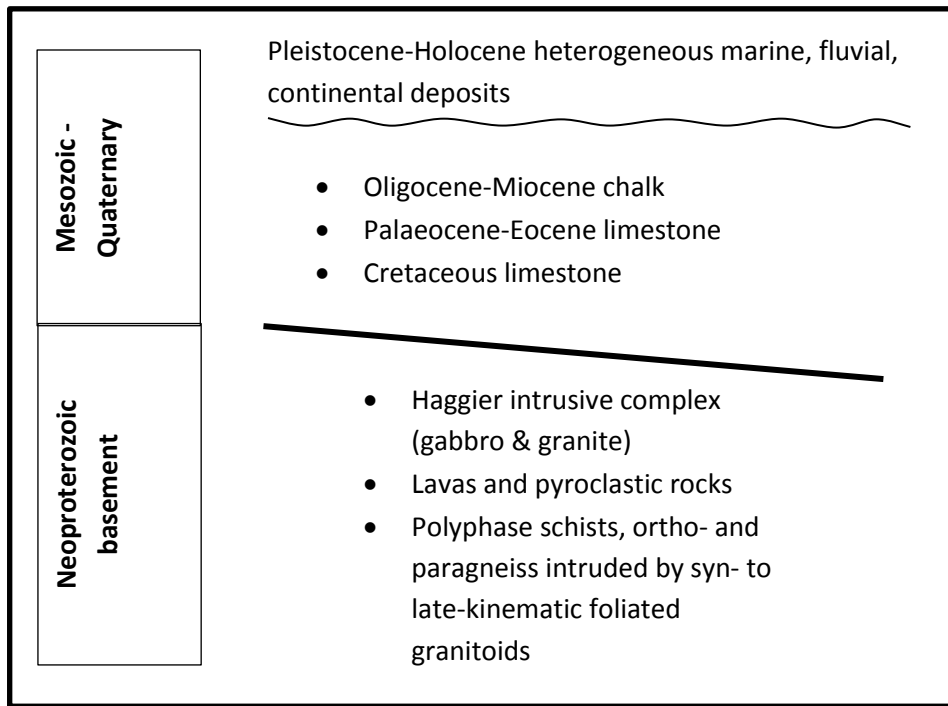


Figure 3- simplified Stratigraphic column highlighting rock sequence of socotra (Beydoun & Bichan, 1969)

The reconstruction of the Gulf of Aden shows that the Socotra Island has occupied, prior to rifting, a position close to the Precambrian Mirbat and Al Halaaniyat Islands outcrops in Oman. This is based on few geochemical and Rb/ Sr whole-rock ages ranging from 850 ± 27 to 706 ± 40 Ma. It is evident that Precambrian rocks of Oman lie within the Pan- African domain and are not part of an older basement such as that identified in eastern Saudi Arabia. The islands sequence of events correlates closely with the Mirbat region of southern Oman. The islands positioning is shown in figure 4 below.

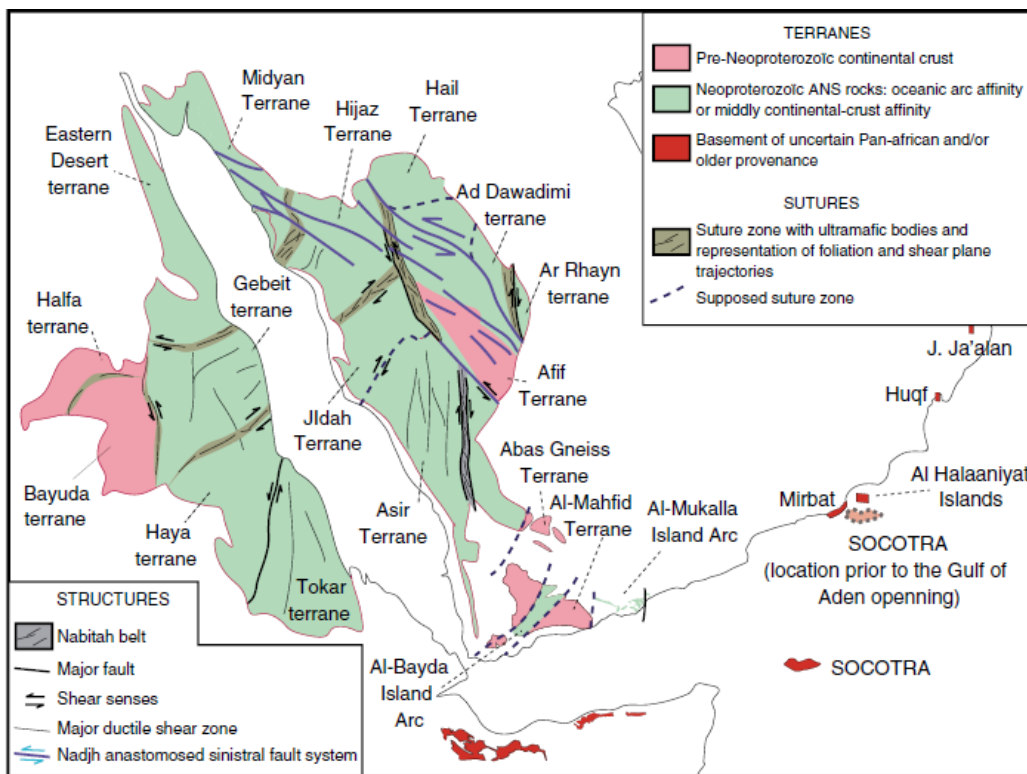


Figure 4– Geological map of terranes in Socotra and the Gulf of Aden (Denèle et al., 2013)

2.4 -Local geological settings

Field relationships



Figure 5- .Fresh cut exposed rhyolite flows near a road on Socotra

In this fresh exposure of rhyolite at a road cutting, several rhyolitic flows can be seen in the figure 5. Also zones of alteration can be identified between flows. The rhyolites in the sequence of geology lie above the mafic volcanics, however the mafic dykes also cross-cut the rhyolites in some sections, it can be inferred that the two were forming at the same time.



Figure 6- Flow banded rhyolite with vitrophyre layer

At the base of the rhyolitic section flow banding can be seen along the contact, this is shown in figure 6. Vitrophyre is also present where the rock has been welded together to form a glass, i.e. obsidian. There is also rubbly material that becomes the contact zone where fluid migration has occurred at the base of the flow. Clasts are also included in the rhyolites that have been picked up from beneath the flow. From the field relationships it is inferred that basalt and rhyolite are present at the same time, i.e.- synchronous.

2.5 Sample collection

The samples used in this study were previously collected on the island of Socotra in 2008. Sample localities are shown in figure 7. The samples were taken from a range of various localities. Samples 39-45 represent a continuous section of flows. The section can be seen to alternate between rhyolite and High silica rhyolites and this will be discussed further in the study. Despite being found at different localities quite some distant apart, the rhyolitic samples are inferred to have the same age. The samples have previously been tested for ages using...with a figure of around 720 ma as a time of formation. Age determinations using secondary ion mass-spectrometry (SIMS) yield an age for the rhyolite of 720 Ma. Overall 14 samples were collected for geochemical investigations. This is a relatively low number of samples which restricts data analysis to a small degree but is enough to provide an insight into Socotran High silica rhyolite. The classification of these samples is discussed later in the study.

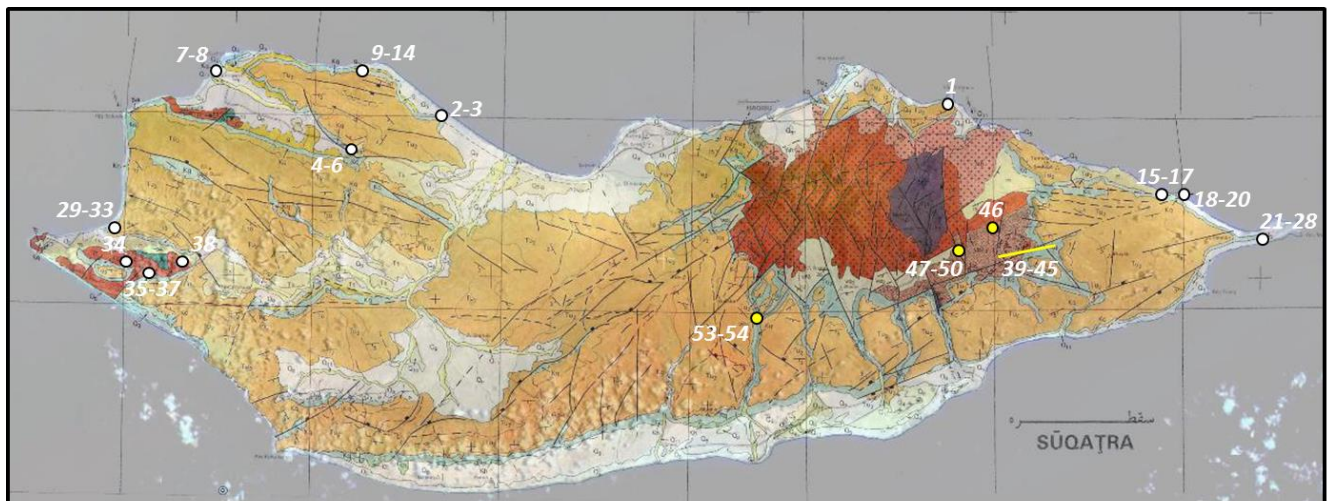


Figure 7- Map showing sampl locations of Socotra study. Sample used in this study are highlighted in Yellow. (Yemen Natural Resources Project 1990, VP)

2.6 Analytical methods and data limitations

The samples collected from Socotra were sampled for whole rock analysis to determine their geochemical composition of rocks. The samples were processed and the data was generated by V. Pease. Whole-rock powders were analysed for major and trace elements using (XRF and LA-ICPMS, Stockholm Univ.). Oxides are reported in wt% and trace elements are reported in parts per million (ppm). Calibrations were made using reference samples and international standards. Overall accuracy and precision is good with standard deviations at around 5% for most trace elements, all show >10% except Cr, which stands at 10.27%. Structurally bound H₂O can be inferred via loss on ignition (LOI).

3 Data analysis

3.1 Classification

The samples collected from Socotra were sampled for whole rock analysis. The geochemical data collected is presented in table 1 on the following page. It is summarized in a series of geochemical plots (Figs. 8-17).

The data represent three distinct compositional groups: The high silica rhyolite (HSR) group (Blue and green), the rhyolite (R) group (Red and orange) and finally the non rhyolitic group (White), made up of an andacite and 2 dacites. This will enable an analysis of the high silica rhyolites but also a direct comparison to the other two groups and covers the range of Socotran volcanism. The groups shown below in figure8 were classified in the groups based on their silica content, as a silica content of >75(wt%) is required.

High silica rhyolite (HSR) group		Rhyolite group		Non rhyolitic group	
Sample	SiO ₂ %	Sample	SiO ₂ %	Sample	SiO ₂ %
SY08-15	75.40	SY08-21	72.70	SY08-41	54.06
SY08-40	78.95	SY08-26	72.06	SY08-47	54.05
SY08-44	79.76	SY08-43	72.47	SY08-53	70.32
SY08-45	77.40	SY08-49	74.94		
SY08-46	76.34	SY08-50	73.27		
SY08-48	79.44				

Figure 8 - 3 distinct compositional groups

It is worth noting that sample number sy08-49 is not considered as part of the HSR group despite the fact that it has an SiO₂ value of c. 75wt%. The focus of this study is specifically on the High silica rhyolite group and determining the formational mechanism.

3.2 Loss On Ignition (LOI)

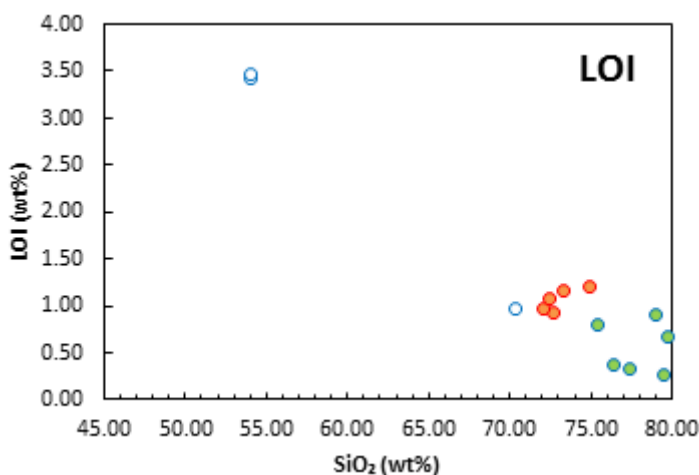


Figure 9 - Loss On Ignition plotted against SiO₂

The geochemical data, in table 2 and figure 9, shows us that the Socotra volcanic rocks preserve different degrees of alteration. The high silica rhyolites can be seen to be the least altered rocks with LOI of less than 1 wt%. It is worth noting that the LOI for both these groups is relatively low with all values >1 wt% showing they are relatively fresh samples, with little alteration. The non rhyolitic group shows 2 members, samples SY08-41 and SY08-47, with LOI ~3.5 wt%. These two samples most likely contain hydrous minerals and minerals formed from alteration, such as hornblende and/or white mica. This is confirmed when studying the petrographic thin sections. These samples may be susceptible to element mobility. . In these samples, only non-mobile elements should be considered. In unaltered rocks both mobile and immobile elements can be used to draw conclusions.

Table 1 – Major and trace element compositions of selected magmatic rocks from Socotra Island

Figure 1.1 - Major and trace element compositions of selected magmatic rocks from socotra island

Sample	SY08-41	SY08-47	SY08-53	SY08-15	SY08-21	SY08-26	SY08-40	SY08-43	SY08-44	SY08-45	SY08-46	SY08-48	SY08-49	SY08-50
Location	Flow	Dyke	Flow	Flow	Dyke	Dyke	Flow	Flow	Flow	Flow	Flow	Dyke	Flow	Dyke
Lithology	An	An	Da	Rhy	Rhy	Rhy	Rhy	Rhy	Rhy	Rhy	Rhy	Rhy	Rhy	Rhy
Group	Non Rhy	Non-Rhy	Non-Rhy	HSR	Rhy	Rhy	HSR	Rhy	HSR	HSR	HSR	HSR	HSR	Rhy
%														
SiO ₂	54.06	54.05	70.32	75.40	72.70	72.06	78.95	72.47	79.76	77.40	76.34	79.44	74.94	73.27
Al ₂ O ₃	17.10	17.12	12.96	13.12	15.56	16.08	11.72	15.31	11.72	11.80	12.09	11.28	14.32	13.87
CaO	5.04	5.82	1.14	0.35	2.16	2.53	0.18	1.14	0.19	0.11	0.23	0.14	1.91	1.37
MgO	4.74	7.16	0.60	0.43	0.63	0.74	0.09	0.97	0.07	0.02	0.09	0.02	0.35	0.51
MnO	0.10	0.15	0.08	0.02	0.02	0.02	0.01	0.03	0.00	0.01	0.03	0.00	0.02	0.04
P ₂ O ₅	0.98	0.11	0.11	0.02	0.04	0.06	0.00	0.06	0.01	0.01	0.01	0.00	0.03	0.04
Fe ₂ O ₃	8.30	8.47	5.52	1.64	1.47	1.46	1.81	1.54	0.72	2.18	2.20	1.24	1.36	2.20
Na ₂ O	5.12	4.76	4.53	4.55	5.99	5.65	2.47	6.97	3.41	4.42	3.68	4.42	5.60	4.48
K ₂ O	2.48	1.15	3.89	4.08	1.17	1.12	4.45	1.28	3.81	3.76	5.04	3.28	1.25	3.80
TiO ₂	1.76	1.06	0.54	0.21	0.17	0.19	0.14	0.19	0.16	0.15	0.17	0.09	0.15	0.26
LOI	0.80	0.92	0.97	3.45	0.90	3.42	0.37	0.33	0.27	1.21	1.16	0.97	1.09	0.68
ppm														
Sc	23.0	31.4	21.2	17.0	16.6	16.6	17.6	16.7	17.1	19.1	13.0	16.6	15.0	15.8
V	84.8	184	16.4	20.5	20.7	29.2	3.67	27.4	6.36	3.70	2.87	8.28	15.7	21.9
Cr	157	197	130	154	180	130	6.87	17.6	9.82	8.20	6.17	9.59	126	122
Ni	97.1	103	11.3	10.6	13.0	13.2	8.99	14.0	10.4	8.28	6.67	9.54	10.2	11.3
Cu	33.6	33.4	10.9	4.89	12.73	34.7	2.81	6.11	3.65	2.91	2.08	11.8	17.5	7.33
Ga	23.0	17.8	28.1	12.5	16.1	17.2	19.5	14.4	18.2	22.6	14.2	19.5	14.5	16.4
Rb	17.6	34.9	70.1	75.4	36	22	87.1	21.3	75.2	68.1	59.7	61.0	55.2	86.1
Sr	1107	469	73.4	129	261	417	24.3	163	36.4	6.18	13.5	15.5	160	154
Y	20	23	86	11	2.2	2.2	50	2.6	45	61	25	58	2.3	31
Zr	286	128	930	98	56	63	313	60	316	479	251	268	68	229
Nb	12.6	2.78	18.7	6.02	1.31	1.21	21.0	0.646	20.3	14.3	8.16	26.9	1.77	7.91
Cs	0.29	3.2	1.1	0.55	0.96	1.2	1.4	0.49	0.580	1.1	0.49	0.17	1.7	0.89
Ba	1200	490	1553	852	173	249	943	237	636	506	397	231	192	889
La	57.2	11.6	45.5	15.9	2.57	3.16	53.1	2.28	36.9	32.6	19.4	24.5	3.32	27.9
Ce	122	24.6	111	34.5	4.39	6.85	65.9	5.71	83.5	75.6	46.3	73.2	6.86	57.6
Pr	14.9	3.23	14.4	3.34	0.546	0.796	14.2	0.713	10.9	10.0	5.51	7.76	0.715	6.50
Nd	59.8	14.8	64.9	12.0	2.477	3.48	60.5	3.00	44.1	44.6	22.9	32.2	2.95	25.4
Sm	9.79	3.64	15.8	2.27	0.640	0.831	13.2	0.729	9.85	10.3	5.02	8.40	0.650	5.47
Eu	2.54	1.23	3.28	0.492	0.233	0.330	1.77	0.263	1.49	1.52	0.755	0.515	0.243	0.789
Gd	6.33	3.86	14.8	1.83	0.575	0.776	12.7	0.692	9.01	10.3	4.41	8.46	0.579	4.79
Tb	0.730	0.625	2.38	0.281	0.077	0.0936	1.78	0.087	1.34	1.66	0.696	1.46	0.0744	0.798
Dy	4.14	4.20	16.2	1.87	0.442	0.485	10.3	0.495	8.53	11.0	4.75	10.6	0.438	5.34
Ho	0.715	0.877	3.28	0.363	0.079	0.0830	1.91	0.092	1.69	2.27	0.954	2.26	0.0761	1.09
Er	1.87	2.54	9.79	1.09	0.183	0.192	5.34	0.220	4.86	6.75	2.83	6.97	0.214	3.36
Tm	0.257	0.367	1.50	0.187	0.0347	0.0342	0.746	0.042	0.702	1.04	0.436	1.10	0.0355	0.498
Yb	1.56	2.42	10.3	1.29	0.180	0.176	4.92	0.193	4.63	6.86	2.92	7.18	0.171	3.46
Lu	0.214	0.334	1.54	0.194	0.0252	0.0227	0.701	0.032	0.654	1.01	0.425	1.03	0.0259	0.504
Hf	6.12	2.97	18.7	2.72	1.45	1.62	8.28	1.55	8.32	11.3	6.02	9.24	1.63	6.05
Ta	0.599	0.177	1.10	0.540	0.0436	0.0419	1.46	0.279	1.40	1.28	0.769	2.01	0.0766	0.637
Pb	10.3	4.09	15.1	22.4	3.21	4.03	13.4	3.34	8.04	8.01	7.31	31.2	5.03	5.52
Th	5.27	1.88	6.16	4.72	0.163	0.383	4.58	0.293	4.43	5.90	4.14	5.90	0.516	8.28
U	0.575	0.358	1.95	1.52	0.09733	0.247	1.44	0.361	1.55	2.00	1.52	2.00	0.226	1.94

3.3 Thin sections-High Silica Rhyolite

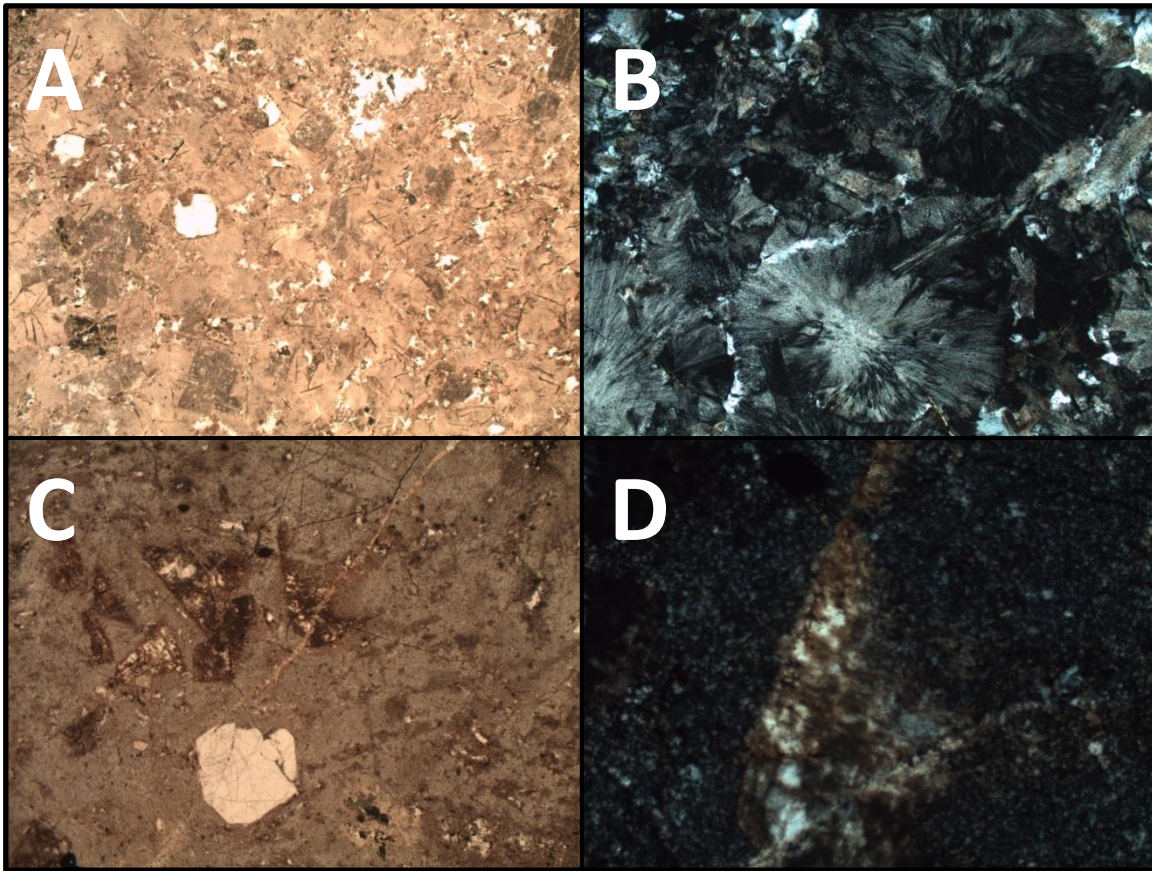


Figure 10(A-D)- Shows 4 different thin section examples from high silica rhyolites. A-Sample SY08-15, typical view of High Silica Rhyolite. B- Example of spherulite. C- Quartz veins and disequilibrium textures of High silica rhyolite. D- X10 view of a broken down crystal undergoing disequilibrium at the time of formation. Slide photographs A and C taken at x4 magnification, B and D at x10 magnification.

The high silica rhyolites have small crystals (0.5mm). These are often formed around a glassy matrix which is hard to identify due to its very fine crystal size. The mineral assemblage consists of quartz, sanidine and plagioclase with epidote and hornblende forming rarer accessory minerals. Samples such as SY08-15 and SY08-45, show igneous textures such as spherulites (figure 10B). These are radiating masses of fibrous crystals in a glassy matrix. These spherulites are probably composed of alkali feldspars and some polymorph of SiO_2 . A common texture observed in these high silica rhyolites are disequilibrium textures (figure 10C and 10D). This indicates that early-formed crystals were unable to completely re-equilibrate with the evolving magma during the later stages of solidification and were reacting with the remaining magma to re-equilibrate to changing P-T conditions at the time that solidification was completed. Minor quartz rich veins are prevalent in some samples. There are phenocrysts present around maximum 1mm in size but in some samples are rare. The rhyolite samples show larger phenocrysts 2mm and show a more defined porphyritic texture in most samples.

4 Geochemical results

4.1- $\text{Na}_2\text{O}+\text{K}_2\text{O}$

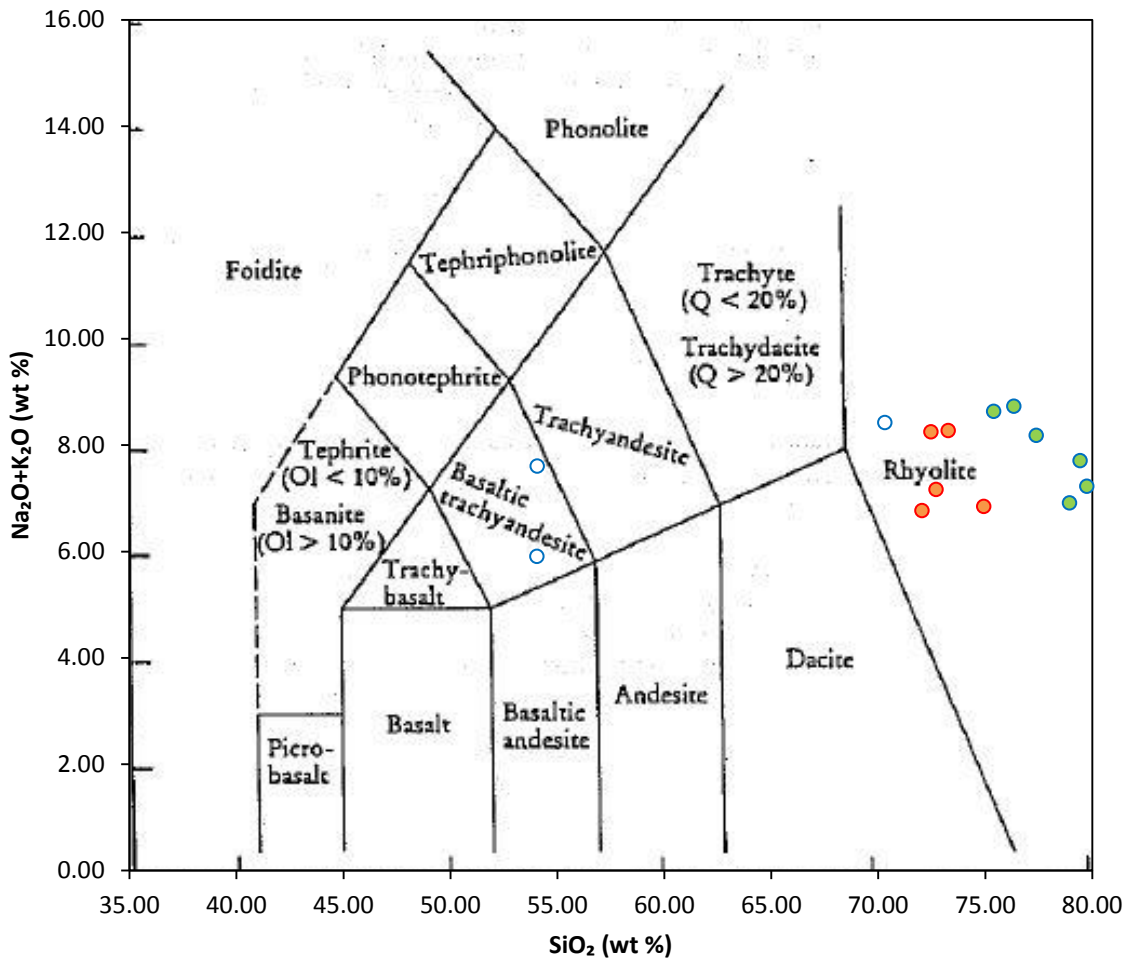


Figure 11 - $\text{Na}_2\text{O} + \text{K}_2\text{O}$ vs SiO_2 classification

From the total alkali-silica diagram (Fig. 11) we can see that the majority the samples plot in the rhyolitic field with an acidic composition. The other two points plot in the Basaltic trachyandesite field but both have high LOI'S so may be altered, questioning their position. According to the SiO_2 vs K_2O diagram in figure 12, all the high silica rhyolite group are calc-alkaline in composition with values of K_2O of between 3-5 wt%. This includes the least evolved end member for the High silica rhyolite group, which is sample SY08-50(part of rhyolite group). It is important to consider the least evolved end member of the HSR group as previously stated. The rhyolite group can all be seen to plot as Arc tholeiitic in composition in exception to SY08-50. Therefore point SYO8-50, shown as the highest rhyolite member in figure 12, will be used as that least evolved end member for the high silica rhyolites. Samples 41 and 47 plots have high LOI values so the classification of these points shown in figure 13 should be used with caution. The samples collected in this study are compared to that of Denele (2013), which is shown in the background. It is clear from this diagram that our two groups of rhyolites are chemically distinct. There is the HSR calc-alkaline group and the Tholeiitic rhyolite group.

4.2 Oxide vs SiO₂ Plots

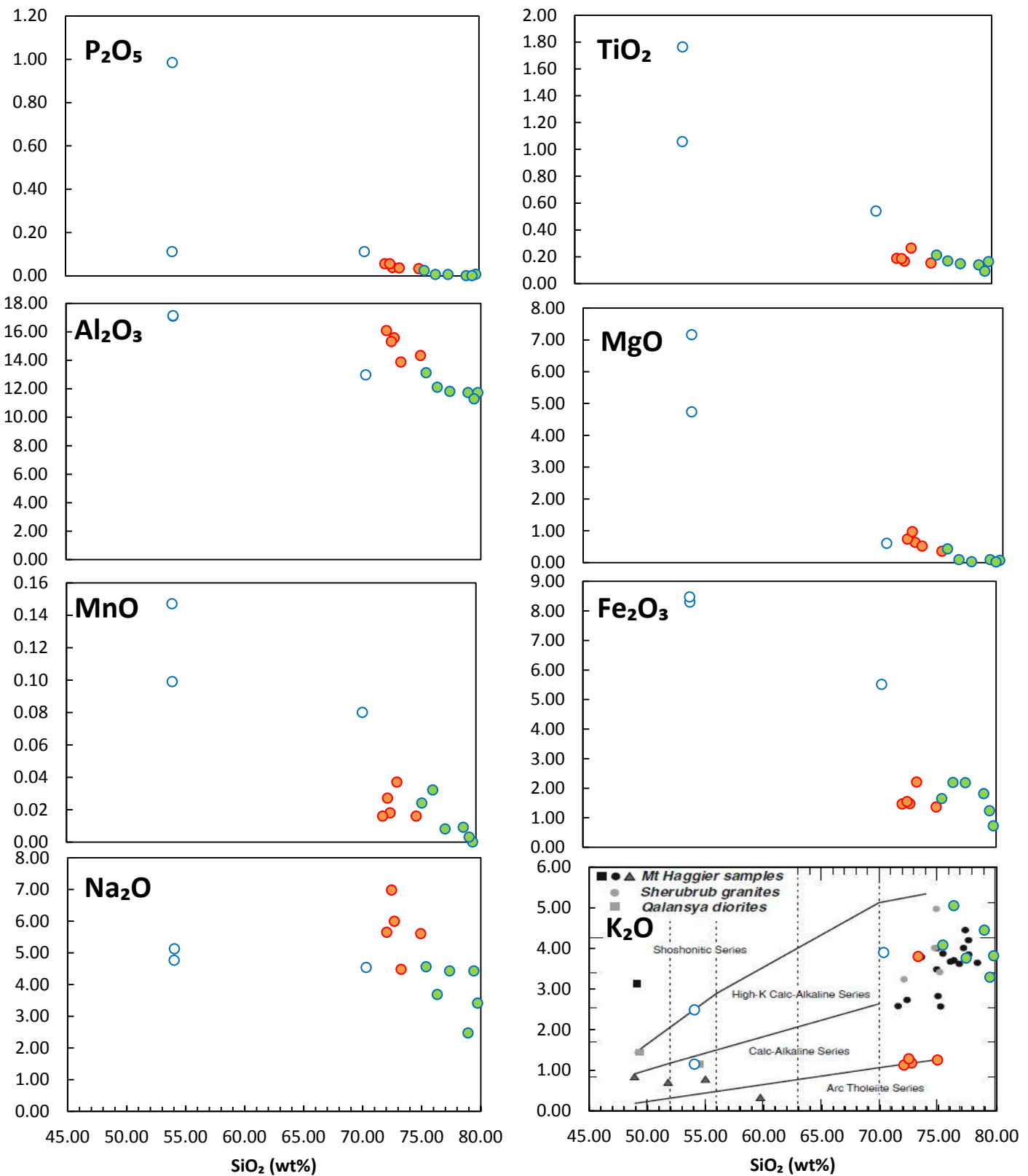


Figure 12- Oxide variation and classification- 3 groups: High Silica Rhyolite(green), Rhyolite (Orange) and Non rhyolitic (White), colours for reference only. Values for oxides are quoted in wt%. K₂O compared to

4.3- CIPW-Normalisation

The chemical analysis of the rock was re-calculated using CIPW norm to give a set of ideal minerals. Modal mineralogy can be difficult to distinguish in fine-grained volcanic rocks, as in this project; hence CIPW-Norm was used. The results of the CIPW norm are shown overleaf in the table 2. The results of the CIPW norm were then used to plot an AFM triangle diagram.

The diagram shows that The HSR and rhyolite samples define extreme members of the calc-alkaline trend (Fig. 11). The non-rhyolites (samples 41 and 47) have high LOI as previously discussed so they should be regarded with caution. The high silica rhyolites approach values of 0 MgO and in the range of 5-10 for Fe. They also show a high alkalinity linked in to the high presence of plagioclases. The Non rhyolitic group shows a relative enrichment in Fe and MgO explained as they have a more mafic composition bearing such minerals as olivine, which takes in Fe and Mg. The 3 points of other group follow a different trend to that of the other group. It is difficult to plot trend to the rhyolites as they are grouped together and the sample number n is low. However, the rock groups belong to two separate series as indicated in figure 12 and 13. The high silica rhyolites plot as calc-alkaline, in figure 12 and 13, and rocks at the end of a calc-alkaline series (Fig. 13). This can suggest that the high silica rhyolites are at the end of a calc-alkaline series, having undergone crystal fractionation to gain increasing silica content along with increasing values of alkaline earths and reducing values of Fe and Mg. The rhyolites plot near the high silica rhyolites however we can determine from figure 13 that they have fractionated from a Tholeiitic series.

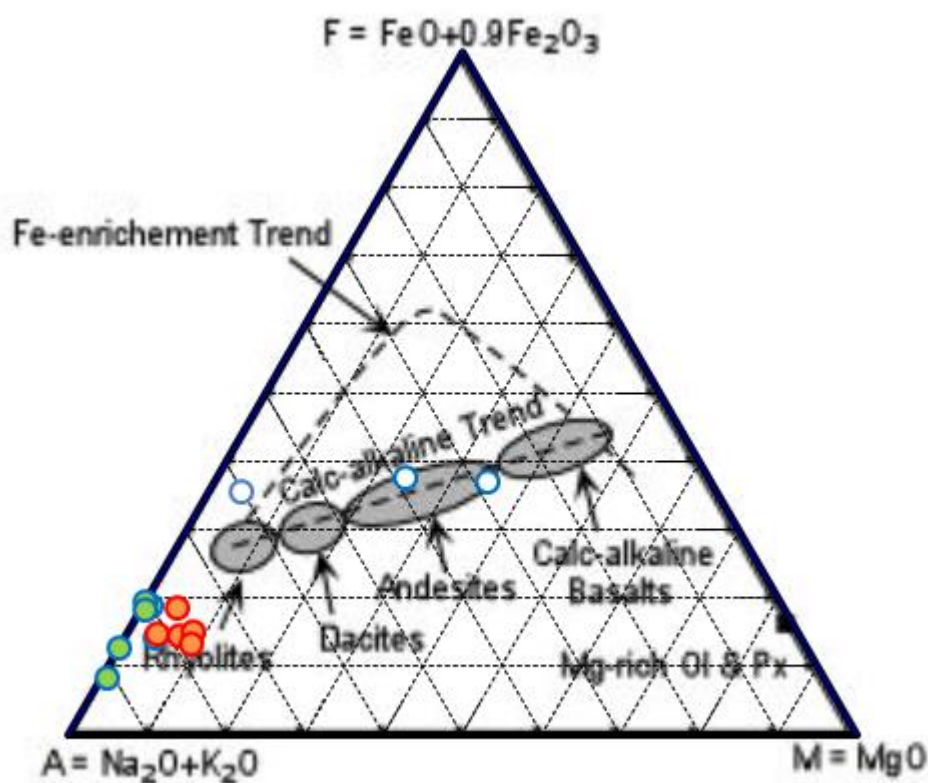


Figure 13- .AFM triangle diagram

Table 2- Results table of CIPW norm, showing normative mineralogy

Minerals	Apatite	Ilmenite	Orthoclase	Albite	Anorthite	Magnetite	Corundum	Diopside	Hypersthene	Quartz	Olivine	Total
SY08-41	2.27	3.34	14.66	43.32	16.35	3.97	0.00	1.82	7.94	0.00	6.20	99.87
SY08-47	0.25	2.01	6.80	40.28	21.95	4.05	0.00	4.99	12.68	0.00	7.03	100.04
SY08-53	0.25	1.03	22.99	38.33	3.54	2.64	0.00	1.20	5.65	24.19	0.00	99.81
SY08-21	0.09	0.32	6.91	50.69	10.45	0.71	0.61	0.00	2.79	27.37	0.00	99.95
SY08-26	0.14	0.36	6.62	47.81	12.16	0.70	1.12	0.00	3.02	28.02	0.00	99.94
SY08-49	0.07	0.28	7.39	47.39	9.28	0.65	0.35	0.00	2.02	32.53	0.00	99.96
SY08-50	0.09	0.49	22.46	37.91	6.51	1.06	0.00	0.02	3.11	28.25	0.00	99.90
SY08-43	0.14	0.36	7.56	58.98	5.26	0.74	0.53	0.00	3.70	22.72	0.00	100.00
SY08-40	0.00	0.27	26.30	20.90	0.89	0.87	2.51	0.00	1.81	46.31	0.00	99.86
SY08-15	0.05	0.40	24.11	38.50	1.61	0.78	0.63	0.00	2.41	31.38	0.00	99.86
SY08-44	0.02	0.30	22.52	28.85	0.88	0.35	1.66	0.00	0.63	44.65	0.00	99.87
SY08-45	0.02	0.28	22.22	37.40	0.48	1.04	0.28	0.00	2.00	36.18	0.00	99.91
SY08-46	0.02	0.32	29.78	31.14	1.08	1.04	0.19	0.00	2.20	34.15	0.00	99.92
SY08-48	0.00	0.17	19.38	37.40	0.69	0.59	0.20	0.00	1.14	40.35	0.00	99.94

4.4- Rare Earth Elements

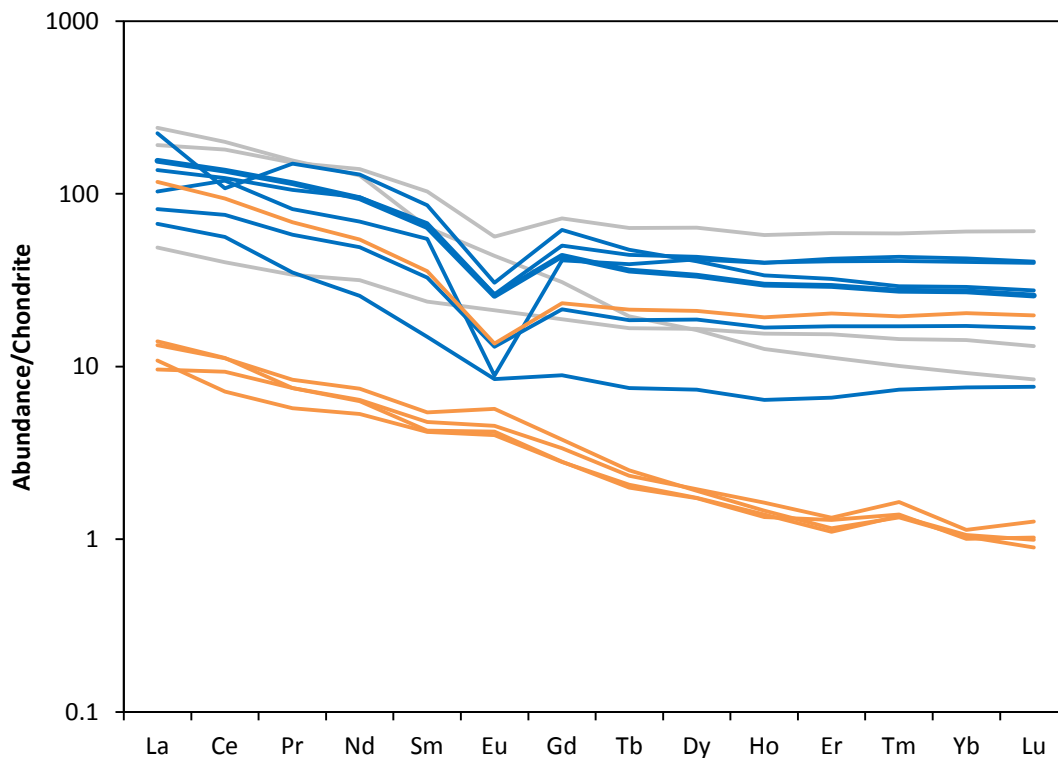


Figure 14 -Rare earth element diagrams. Chondrite normalised values after sun and McDonnagh (1989) Pm not measured in analysis. Rhyolite group plotted in orange and High silica rhyolite in blue. Non rhyolitic members are faded out to grey

Chondrite normalized values of all the samples show different patterns. The pattern observed by the High silica rhyolite group is similar to high silica rhyolites described in Glazner. Et al. (2008), which is described as a seagull pattern. The High silica rhyolites overall show an enrichment in all REE's, except Eu, which is to be expected (Glazner. Et al. 2008). It is clear from the diagram that the HSR group has a distinct depletion pattern for Eu. This depletion is not present in the normal rhyolite group. This Eu depletion is shown by negative values for Eu/Eu^* ratios in the range of -0.061-0.160, whereas the rhyolite group plots positive figures. The High silica rhyolites are generally equally in REE's enriched with values of $[La/Lu]_n$ of 3.45-8.7. This is shown by relatively stable line patterns, with a slightly less enriched Heavy REE. However the rhyolite group shows a depletion in the Heavy REE's with for $[La/Lu]_n$ of 11-13.74. No depletion in HREE'S suggest no garnet suggesting a shallow mantle source, suggesting the source is not of mafic origin. Sample SY08-50 is the orange line that plots in the high silica group. It becomes more apparent that this is perhaps a least evolved end member related to the high silica rhyolite group. It is worth noting that Pm is not included in this plot as it was not tested for during geochemical analysis. It is worth noting that the pattern expected for Ce is usually smooth however two sample numbers 44 and 48, show an enrichment and depletion, this is most likely due to an analytical error, however Ce does have two oxidation states so it cannot be ruled out that these depletions and enrichments are real.

4.5 Multi element plot

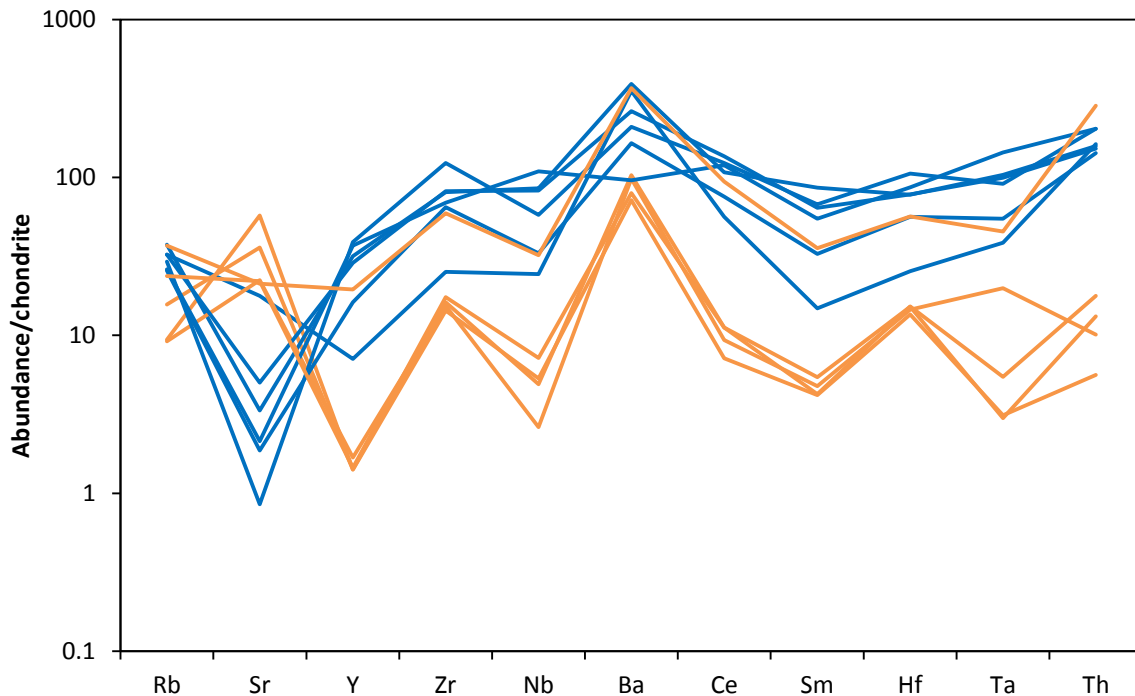


Figure 15 –Multi element plot. Chondrite normalised values after sun and McDonnagh (1989) Rhyolite group plotted in orange and High silica rhyolite in blue.

From the multi element plot we can see that again the two groups of High silica rhyolites and rhyolites are separated again. They both show different patterns in figure 15. For some elements the rhyolites show the same signature but with a decreased value, for example Ba. However for some elements the two are very distinguished. These include Rb, Sr and Y which are the most prominent. Ta also shows a different trend but this will not be considered. In the case of Sr, the rhyolites show enrichment whereas the HSR show a depletion of Sr. The HSR's show a higher value of Y when compared to the rhyolites which show a depletion. Sr, Y and Rb have been selected for further study and which is shown in the following pages. The orange line that plots with the high silica rhyolites is again sample SY08-50, it is becoming evident that this may be a member of the high silica rhyolite group despite the fact it has lower silica than required as it always follows a similar pattern. This will be discussed later in the study.

4.6 Europium

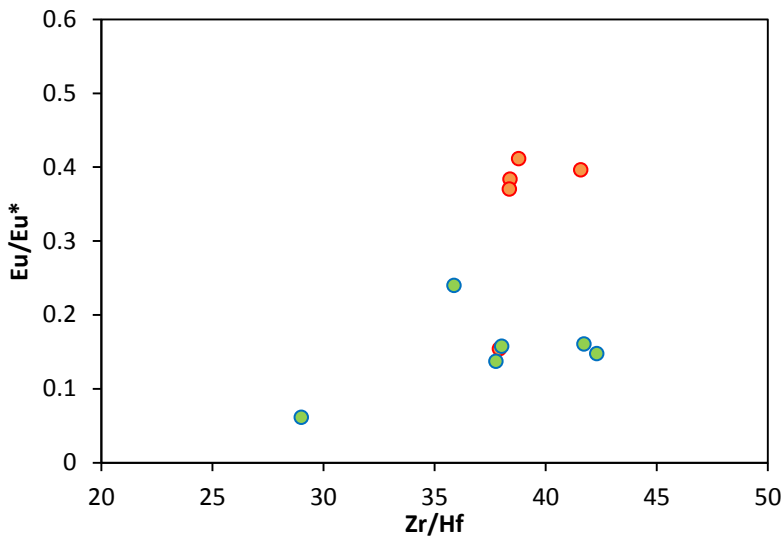


Figure 16 –Eu/Eu* v Zr/Hf

Plagioclase crystal fractionation causes sharp declines in Ba and Eu/Eu* as compositions get increasingly more silica rich. Zr/Hf plots the points in figure... are semi-constant (34-43) and plot close to the chondritic mark value of 40. Zr/Hf is most commonly a fixed point as most materials show near chondritic values, as Zr/Hf behaves identically in almost every Earth system. It can be seen for this fixed point that there are variations in Eu/Eu*. These are nicely divided between the High silica rhyolite group and the rhyolite group with the exception of Sample SY08-50. Eu/Eu* vs Zr/hf illustrates plagioclase crystallisation. The two groups have different amounts of plagioclase crystallisation. The Eu anomaly shown, of 0.15 to 0.4 is high relative to Zr/hf.

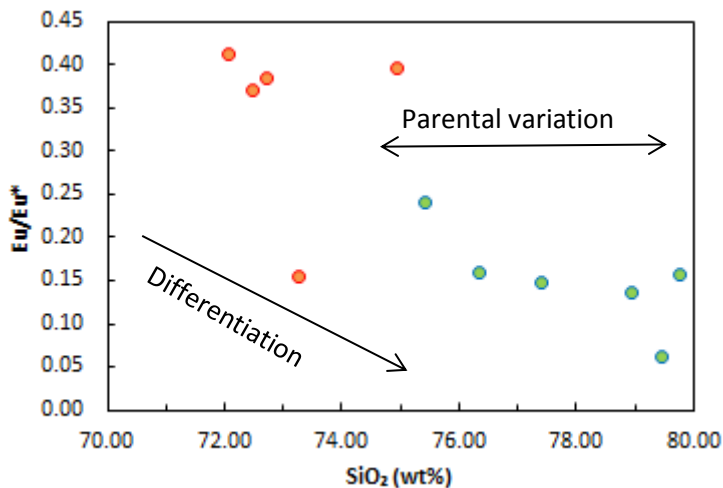


Figure 17- Eu/Eu* vs SiO₂

So they show varying degrees of differentiation... the high silica rhyolite cover a small range of Eu/Eu* values and all rhyolites show that they are quite evolved due to their low Eu/Eu* values. The samples again define two distinct groups in figure... The high silica rhyolite group shows varying levels of of siO₂ with a relatively fixed composition of Eu/Eu*. This shows that the magmas have possibly evolved from differential parental melts. However it is possible to apply a weak fractionation trend to the whole diagram as the Eu gap is relatively small. However this is unlikely

and the number of samples is too few to reach any drastic conclusions. Overall it is most likely that they have different origins and form by different processes.

5. Discussion

5.1 Sample classification

The geochemical data is presented as 3 groups: The high silica rhyolite (HSR) group, the rhyolite (R) group and the non-rhyolitic group. However when looking at the various geochemical plots it is evident that data samples SY08-49 was correctly plotted with the Rhyolite group, despite the fact this sample has a SiO₂ content of 74.94 (wt%). This is seen as it consistently plots with the Rhyolitic group in all figures. However it can also be seen that sample SY08-50 has different chemical affinities. Sample- 50, despite having relatively low SiO₂ value (only c. 73 wt%) and HSR usually need a value of >75 (wt%) consistently has the chemical characteristics HSR, for example Eu depletion with REE enrichment and Higher Rb/Sr values. For the purposes of this discussion sample- 50 is now considered a member of the high silica rhyolite group. Sample -49 is considered to be a member of the rhyolite group. This makes the following groups as follows (fig. 18).

High silica rhyolite (HSR) group		Rhyolite group	
Sample	SiO ₂ %	Sample	SiO ₂ %
SY08-15	75.40	SY08-21	72.70
SY08-40	78.95	SY08-26	72.06
SY08-44	79.76	SY08-43	72.47
SY08-45	77.40	SY08-49	74.94
SY08-46	76.34		
SY08-48	79.44		
SY08-50	73.27		

Figure 18 – Revised: 2 distinct compositional groups

5.2 Geochemical groups

5.2.1 Sr v Y

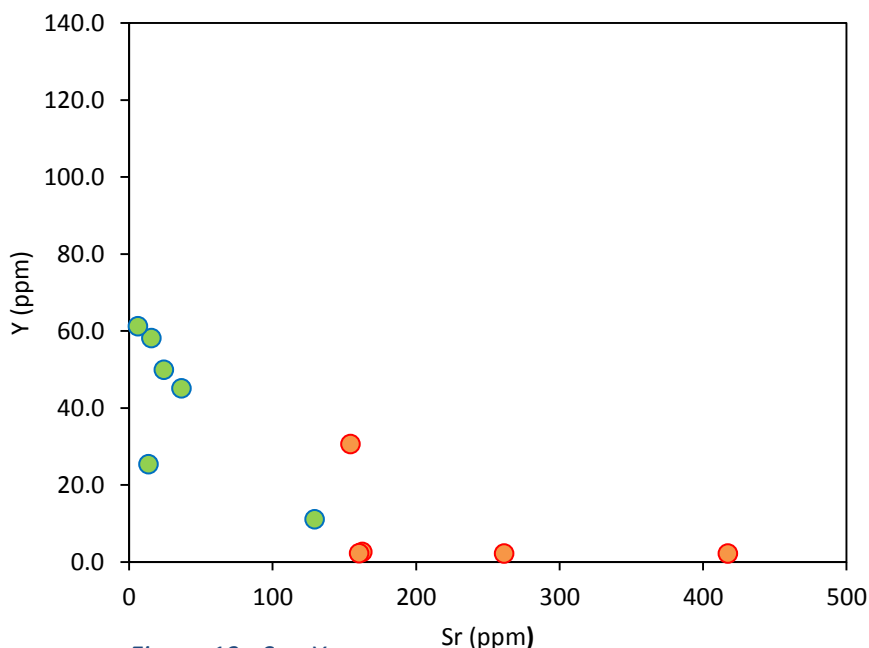


Figure 19 – Sr v Y

It can be seen from the graph The HSR's show little variation in Sr (7-30 ppm) as Y varies from 25 to 60 ppm, with the exception of point 15 (and 50). Y enrichment is a property of HSR's as they are generally enriched in REE's (Glazner Et al. 2008). Y generally behaves as a Heavy REE so is enriched in the high silica rhyolites. The HSR also shows a depletion in Sr which is to be expected (Halliday 1991)(Glazner Et al 2008). This is because although Sr is incompatible it is partitioned and can substitute for Ca and K for a variety of minerals as it fractionates at mid-stage during magmatic processes. Thus Sr tends to be enriched in intermediate rocks. This is the pattern displayed by the rhyolitic group which has high yet varying values for Sr (150-450 ppm) with very low values of Y <5ppm. The low values for Y can be explained as it is strongly partitioned into hornblende and biotite which show higher concentrations in the rhyolitic rocks. In contrast the dacite would have plotted a value of 1107 ppm due to its even higher concentrations of these minerals. Yttrium displays very low mobility under all conditions so is concentrated more in the HSR. This plot shows that the rhyolites have a low Y and high Sr values, these therefore cannot be related to the High Silica rhyolite formations and therefore they MUST have a different origin.

5.2.2 Rb vs Sr

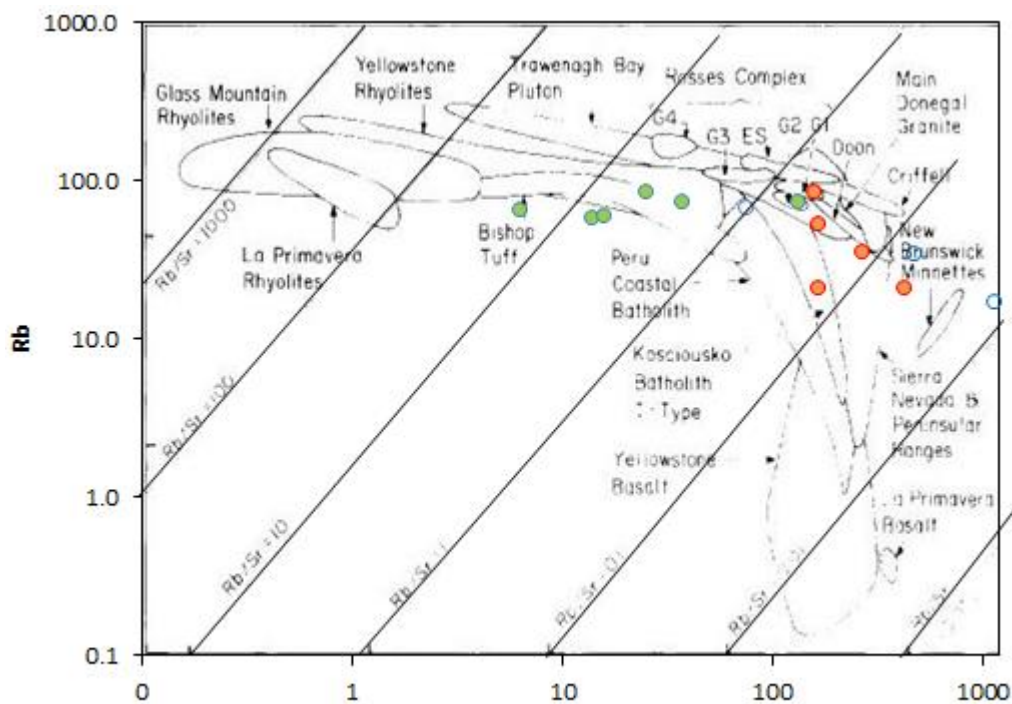


Figure 20 – Rb V Sr showing Rb/Sr ratios Sr

The Rb v Sr diagram shows us again that there are two distinct groups forming with different origins. The High silica rhyolites show a very similar pattern with higher ratios of Rb/Sr. The High silica rhyolites plot on a horizontal trend, whereas the rhyolites have a negative trend which shows that they have different origins. The fact that Rb can substitute for K but only in minerals such K-feldspar such as microcline and orthoclase which is potentially why there is variation shown in the rhyolite samples with a range of values. However, because Rb has a larger ionic radius it behaves incompatibly and it becomes concentrated in late stage differentiates such as the high silica magmas, thus ratios of Rb/Sr increase with magmatic evolution. HSR therefore have higher Rb/Sr

ratios as rb more incompatible than sr in nearly all magmatic systems (Halliday 1991). The diagram shows us that the HSR are much more evolved than their rhyolitic counterparts.

The high Rb/Sr ratio (fig) and very low Sr (fig) also tells us that the High Silica Rhyolites cannot have formed by partial melting involving typical crustal sources. Sr is generally incompatible as a LILE, so if the hsr formed using the partial melting model we would expect them to be enriched in the melt. The very low values displayed tell us that HSR cannot be formed directly from partial melting of mafic rocks and supports the fractional crystallisation mush model (Bachmann and Bergantz). Overall it has now been established that there are two groups and we have also that they are forming by different processes and have different origins.

5.3 Formational processes

5.3.1 Rare earth elements-revisited

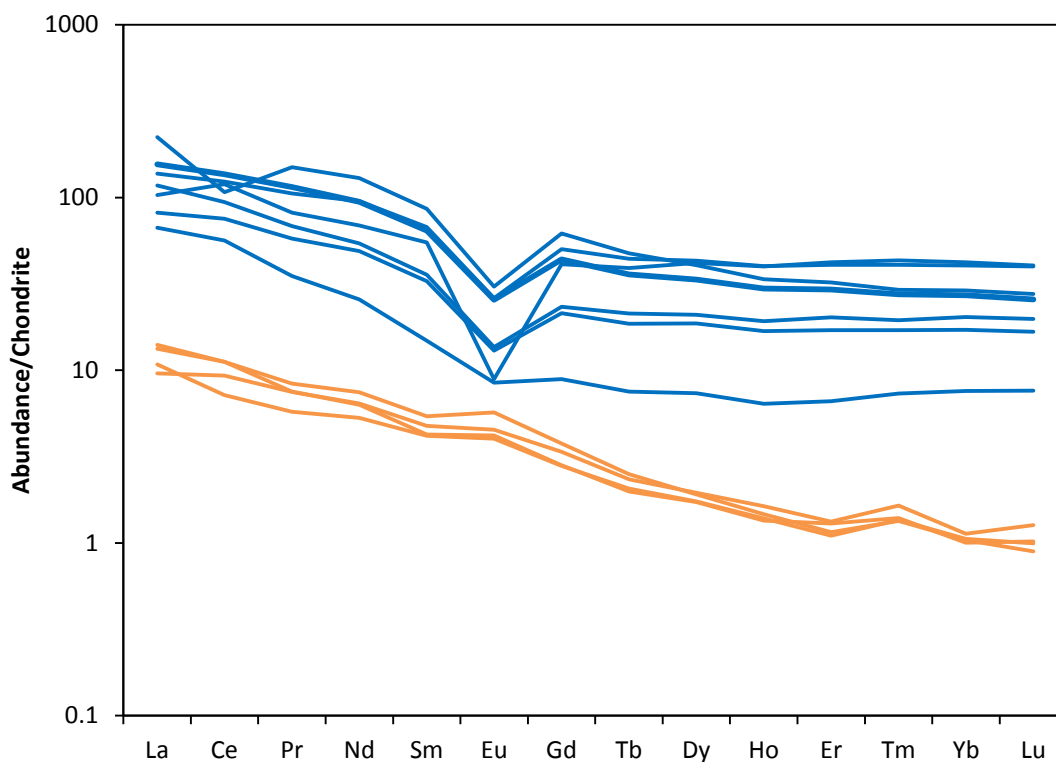


Figure 21- Revised Rare earth element diagram. Chondrite normalised values after sun and McDonough (1989). Rhyolite group plotted in orange and High silica rhyolite in blue.

The REE diagram has now been revised to show that sample 50 does in fact belong to the high silica rhyolite group. The Eu depletion pattern shown by the high silica rhyolite group is explained as the crystallisation of plagioclase in the mush. As plagioclase is fractionating out it takes up Eu from the melt, as Eu has an affinity for plagioclase. The formation of plagioclase is a crucial element to this study (Bachman and Bergantz 2004) (Streck and grunder 2008). The lack of this Eu depletion in the non-high silica rhyolites indicates that plagioclase was not fractionating out in the mush. This shows

that the two are forming by different processes and different origins. This is reinforced by different REE patterns overall, with the rhyolites showing a depletion in heavy REE's.

It can be concluded from the figures 19-21 that the High silica rhyolites must have evolved using the Bachman and Bergantz (2004) melt mush model. This is due to the fact that it has the following characteristics; Firstly it shows an enrichment in all REE's with the exception of a Eu depletion. This Eu depletion shows that plagioclase is fractionating out of the melt which is not possible for the mafic model. Furthermore it also has depletions in Sr, Ba and Eu. These are incompatible elements, so if the HSR formed using the partial melting model we would expect them to be enriched in the melt, so therefore be in high quantities with the high silica rhyolites forming. This is obviously not the case so it is concluded that the HSR cannot form via the partial melting of mafic rocks and must follow the fractional crystallisation model.

5.3. 2 Formational Model

Having concluded that the High silica rhyolites form using the Melt-mush extraction model, proposed by Bachman and Bergantz (2008), their origin can now be discussed.

The high silica rhyolites need to have evolved in a magma chamber where plagioclase is fractionating to create a mush of 40-50% crystallinity. However plagioclase will most likely rise to the surface of a chamber as it will have a lower density than the overall melt. Furthermore from the field relationships we can see that the rhyolites are interacting with the high silica rhyolites. Sample 39-45 (Fig. 7) were taken from a range of various localities. Samples 39-45 represent a continuous section of flows. The section can be seen to alternate between rhyolite and High silica rhyolites. This is simplified and shown in the following diagram.

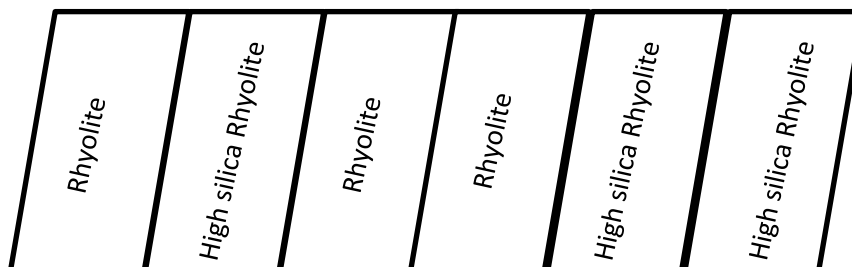


Figure 22 –Simplified continuous flow section, altering in composition.

From the field relationships we can see that rhyolites co-exist with mafic rocks and also lower silica rhyolites. A model is required that allows the generation of rhyolites intermittently between High silica rhyolites, or vice versa. A popular explanation for such criteria is a stagnant cap model. Bachmann and Bergantz (2004) (fig. 23).

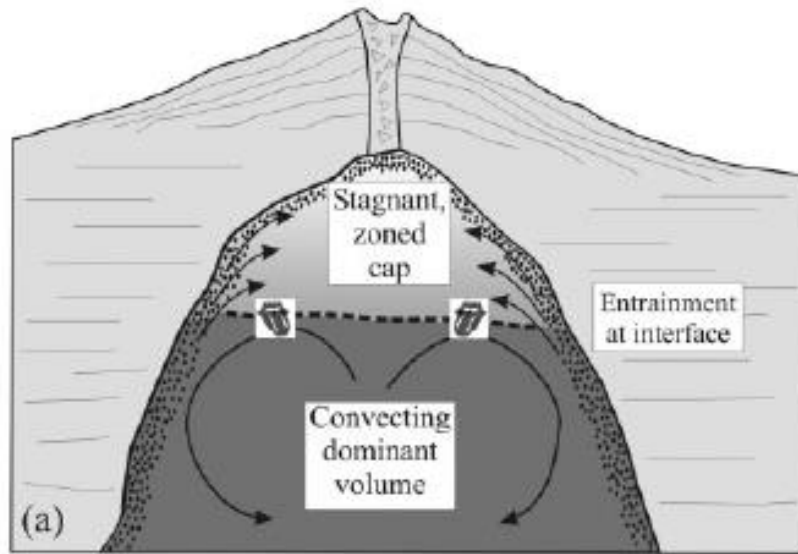


Figure 23–Stagnant cap model (Bachmann and Bergantz 2004)

In this model plagioclase can crystallise at the roof of the chamber. Trapped between plagioclase crystals lies the interstitial melt which has a high silica rhyolite composition. When crystallisation has occurred over a period of time, 40-50% crystallinities can be reached. This would stop convection occurring in the upper regions of the chamber, thus creating a stagnant cap. The still convecting lower chamber will be of rhyolitic composition. This will need to build up over time as large volumes in the magma chamber are required to form high silica rhyolites (Halliday 1991). Overtime the interstitial melt may percolate upwards, as described by Bachman and Bergantz (2004), forming a high silica rhyolite horizon. Eventually enough pressure builds up for there to be an eruption at which point the high silica melt will be erupted to form volcanic high silica rhyolitic rocks. Following this eruption, normal rhyolitic eruptions will occur. This is what can account for the variation in flow composition present in the field. The overall model implies a stagnant cap overlying the convecting, denser parent magma to explain its co-existence with rhyolitic flows.

6 Conclusion

The high silica rhyolites and rhyolites of Socotra have different geochemical signatures. The high silica show a calc-alkaline composition and trend whereas the rhyolites show a more tholeiitic composition. The high silica rhyolites show characteristics of classic high silica rhyolites around the world. This is; A depletion in Eu, Ba and a significant Sr depletion. A SiO₂ value of >75 wt%. They also show high Rb/Sr ratios and are generally enriched in REE's. They are shown to be chemically distinct from the normal rhyolites. The high silica rhyolites of Socotra follow the Bachmann and Bergantz (2004) melt-mush extraction model. This is evident as they show significant Eu depletion and that plagioclase was crystallising out of the melt. They most like formed from a stagnant cap within a rhyolitic magma chamber shown in figure 23. Further research into the Socotran rhyolites should use a greater number of samples and a wider range of samples, including more mafic orientated rocks to show more trends and mineral associations. Isotope data can also be used for investigation into Nd and Sr to allow further understanding of the high silica rhyolites history. Also numerical modelling could be conducted to see if HSR can be derived from least to most evolved samples.

7 Reference list

- Allen, A.S.R., Morgan, D.J., Wilson, C.J.N., Millet, M-A., 2013. From mush to eruption in centuries: assembly of the super-sized Oruani magma body. *Contributions mineral petrology* 166: 143-164
- Beydoun, Z.R. and Bighan, H.R. 1969. The geology of Socotra, Gulf of Aden. *Quarterly journal of the geological society*, v.125: 413-441
- Denele, Y., Leroy, S., Pelleter, E., Pik, R., Talbot, J-Y., Khanbarri, K., 2013. The cryogenian Arc formation and successive high calc-alkaline plutons of Socotra island (Yemen). *Frontiers in Earth Sciences*: 335-360
- Frost, B.R., Barnes, C.G., Collins, W.J., Arculus, R.J., Ellis, D.J., Frost, C.D., 2001. A geochemical classification for granitic rocks. *Petrology* 42; 2033-2048
- Glazner, A.F, Coleman, D.S, Bartley, J.M., 2008. The tenuous connection between high silica rhyolites and granodioritic plutons. *Geology*, 36; 183-186
- Halliday, A.N, Davidson, J.P, Hildreth, W, Holden, P., 1991. Modelling the petrogenesis of high Rb/Sr magmas. *Chemical geology*, 92; 107-114
- Leroy, S., Gente, P., Fournier, M., D'Acromont, E., Patriat, P., Beslier, M-O., Bellahsen, N., Maia, M., Blais, A., Perrot, J., Al-Kathiri, A., Merkouriev, S., Fleury, J-M., Ruellan, P-Y., Lepvrier, C., Huchon, P., Et al. 2004. From rifting to spreading in the eastern gulf of Aden: a geophysical survey of a young oceanic basin from margin to margin. *Terra Nova* 16: 185-192
- Linnen, R.L. and Keppler, H., 2002. Melt composition control of Zr/Hf fractionation in magmatic processes. *Geochimica et Cosmochimica Acta*, V 66:3293–3301
- Macdonald, R, Davies, G.R., Bliss, C.M., Lea, P.T., Bailey, D.K., Smith, R.L., 1987. Geochemistry of High silica peralkaline thylolites, Naivasha, Kenya rift valley. *Petrology* Volume 28; 979-1008.
- Mason, B.G., Pyle, D.M., Oppenheimer, C., 2004, The size and frequency of the largest explosive eruptions on earth: *Bulletin of volcanology*, v66: 735-748.
- Pease, V and Persson, S., 2003. Neoproterozoic island arc magmatism of northern Taimyr. *Dept. of Geology and Geochemistry*, Stockholm University, SE106 91
- Rantakokko, N., Whitehouse, J.M., Pease, V., Windley, B.F., 2014. Neoproterozoic evolution of the eastern Arabian basement based on a refined geochronology of the Marbat region, Sultanate of Oman. *Geological society London, Special publications*, V392:107-127
- Siebel, W., Schmitt, A.K., Kiemele, E., Danisik, M., Aydin, F., 2011. Acigöl rhyolite field, central Anatolia (part II): geochemical and isotopic (Sr–Nd–Pb, $\delta^{18}O$) constraints on volcanism involving two high-silica rhyolite suite. *Contribution mineral petrology* 162: 1233-1247
- Streck, M.J and Grunder, A.L., 2008. Phenocryst poor rhyolites of bimodal, tholeiitic provinces: the rattlesnake Tuff and implications for mush extraction models. *Bull volcano* 70: 385-401

Sun,S. and McDonough,W.F., 1989 Chemical and isotopic systematics of oceanic basalts:implications for mantle composition and processes. *Geological Society, London, Special Publications*; v. 42; p. 313-345

Vazquez, J.A and Ried, M.R. 2002. Time scales of magma storage and differentiation of voluminous high silica rhyolites at Yellowstone caldera, Wyoming. *Contribution mineral petrology* 144: 274-285